Comparison of Organic Acid-based Organosolv Lignins Extracted from the Residues of Five Annual Crops

Nadja Cachet and Bouchra Benjelloun-Mlayah *

Organosolv lignins were extracted from corn stover, wheat, rice straw, reed straw, and sugarcane bagasse using a mixture of acetic and formic acids, at relatively low temperature and atmospheric pressure. Lignin content, residual carbohydrates, ash levels, proteins, and molecular weights were determined in each extracted lignin. The lignin content of all samples was relatively high, confirming the performance of the pretreatment process. The low molecular weights were in a narrow range, in accordance with the organosolv lignin molar masses. However, some differences between studied lignins were highlighted, in particular in rice straw lignin, which contained the highest silica, calcium, and nitrogen contents. Nuclear magnetic resonance spectroscopies (^{31}P and semi-quantitative Heteronuclear Single Quantum Correlation) underlined the structural similarities and differences between these organosolv lignins. Corn stover and sugarcane bagasse lignins were rich in non-methoxylated (H-Unit) or mono-methoxylated (G-Unit) phenolic units, making them the best promising candidates for production of phenolic resins. Wheat straw lignin was richer in aliphatic OH than in phenolic OH. This is an advantage for use as polyol substitute in polyurethane synthesis. Reed straw lignin was less specific, with a balanced content of OH groups. However, it contained a high concentration of β-O-4 linkages, which is favorable for depolymerization.

Keywords: Lignin; Organosolv process; NMR; Characterization; Annual plant; Organic acids

*Contact information: Compagnie Industrielle de la Matière Végétale (CIMV), 109, Rue Jean Bart – Diapason A, 31670 Labège, France; *Corresponding author : b.benjelloun@cimv.fr*

INTRODUCTION

In the last 10 years, governments and researchers have shown an increasing interest in biorefineries as an alternative to our strong dependence on fossil fuels. The biorefinery, based on the oil-refining model, can be defined as a sustainable processing of biomass into a spectrum of marketable products, including second-generation biofuels, chemical intermediates, polymers, and materials (*e.g.*, carbon fibers) (Poveda-Giraldo *et al.* 2021). The usage of lignocellulosic biomass depends on its optimized fractionation into its three major constituents, *i.e.*, cellulose, hemicellulose, and lignin. Among the different pretreatment processes employed to achieve this target, the organosolv process is the most promising one (Thoresen *et al.* 2020). Organosolv pretreatment can occur in a large range of organic or aqueous–organic solvent systems with or without added catalysts in the temperature range between 100 and 250 °C. When organic acids are used for the fractionation of biomass, the major chemical reactions involve the cleavage of β-O-4 linkages in lignin, its condensation, and the esterification of a part of its OH groups. Thus, the lignin dissolved from acetic acid fractionation contains more acetyl groups in Cα and Cγ position compared to milled wood lignin (Li *et al.* 2016)

The Compagnie Industrielle de la Matière Végétale (CIMV, Paris, France) has developed an innovative organosolv process using a mixture of acetic and formic acid, at relatively low temperature and without the use of a catalyst. The acid mixture can solubilize efficiently the lignin during the pretreatment due to the values related to the Hildebrand's solubility parameters of the acid mixture (12.1 for the formic acid, and 10.1 for the acetic acid) (Pan and Sano 1999). This pretreatment process allows an efficient fractionation of biomass and the extraction of almost all lignin without apparent product degradation (Banoub *et al.* 2007; Snelders *et al.* 2014).

Lignin is the second most abundant natural polymer available in nature, accounting for 15% to 40% of the biomass. It is widely accepted that biosynthesis of lignin takes its origin from the polymerization of three types of phenylpropane units: *p*-coumaryl, coniferyl, and sinapyl alcohols. They are present in different quantities, depending on the origin of the plant material. Their oxidative enzymatic polymerization leads to the *p*-hydroxyphenyl, guaiacyl, and sinapyl units found in lignin structure (Ralph *et al.* 2004). The current trends have shown that lignin may be a good alternative for feedstock of phenol-derived products, even the replacement of petrochemical-derived aromatic monomers, technical carbons, fuels, and adhesives (De Souza *et al.* 2020). Nevertheless, technical lignins' physico-chemical properties highly depend on their extraction process (solubility, sulfur content, molecular weight for instance), and on the original feedstock (Watkins *et al.* 2015). Thus, the use of technical lignins for industrial applications is still challenging today (Vishtal and Kraslawski 2011).

The present work aims to extract lignin fractions from five different raw materials using the organic acid-based organosolv pretreatment. A further goal is to perform a complete characterization of these fractions to determine their composition and their functionality. A deep knowledge of chemical structure and properties is essential to evaluate the lignin potential in applications and to optimize its valorization. This study focused on five straws of annual crops widely available: corn stover, wheat, rice and reed straws, and sugarcane bagasse. A comparison of these different organosolv lignins was made to estimate the influence of the raw material on lignin characteristics. Choosing a pre-industrial organosolv process to extract the five studied lignins could be helpful for the manufacturing of future value-added lignin-based products.

The composition and structural features of these lignins were analyzed by common analytical methods, such as elemental analysis, gel permeation chromatography (GPC), and Klason lignin assessment. In addition, nuclear magnetic resonance (NMR) spectroscopies (^{31}P and semi-quantitative Heteronuclear Single Quantum Correlation (HSQC)) helped highlight the similarities and differences between these lignins extracted from different annual crops.

EXPERIMENTAL

Materials

The lignin-rich fractions (called Biolignin^{TM}, a trademark of CIMV organosolv lignin) (Compagnie Industrielle de la Matière Végétale, Paris-Neuilly, France) were extracted from five raw materials using an organic acid-based pre-treatment process (Delmas *et al.* 2006; Delmas 2008; Delmas *et al.* 2011; Benjelloun-Mlayah and Delmas 2019).

The crops residues were firstly mechanically prepared, cut in *ca.* 5 to 10 cm long stems and dedusted. The lignocellulosic materials were then fractionated in a mixture of acetic acid (AA) (PanReac, 99.5%, Barcelona, Spain)/formic acid (PanReac, 98%, Barcelona, Spain) (FA)/water (H_2O) (55:30:15, w/w/w) during 3.5 h at 105 °C, at atmospheric pressure. The extraction liquor, containing the lignin and the hemicelluloses, was then concentrated at 65% dry matter, and the lignin was precipitated by adding water to the concentrated liquor. The lignin-rich fraction, (Biolignin™), was finally recovered by filtrating the above suspension and washing the solid with water (50 °C).

Each feedstock was fractionated at least five times under the same fractionation conditions, to extract five different samples of Biolignin™. Each sample was analyzed. The results reported in this study are the average values obtained from the five lignin fractions of each feedstock. The same extraction conditions were used, whatever the raw material, in order to evaluate the efficiency of the pretreatment on the studied feedstock. Depending on the result, *i.e.*, extracted lignin yields, the optimization of the process parameters, such as the temperature and/or the extraction duration, can be considered.

In the following, the lignin-rich fractions were named CS, RS, WS, ReS, and SB Biolignin™ for, respectively, lignin extracted from corn stover, rice straw, wheat straw, reed straw, and sugarcane bagasse.

Ash Content

The ash content was determined according to the procedure detailed by Sluiter *et al.* (2008a). The ash content of Biolignin™ was gravimetrically determined after a furnace calcination at 575 °C ± 25 °C during 24 h.

Elemental Analysis and Protein Content

Elemental analyses were performed on a PerkinElmer 2400 Series II CHNS/O elemental analyzer (Waltham, MA, USA). A total of 2.0 mg (+/- 0.5 mg) of sample were weighed. Only C, H, and N elements were analyzed.

The protein content from every lignin material was deduced from the nitrogen's (N) percentage using the nitrogen-to-protein conversion factor. This factor is 5.4 (wheat straw), 5.62 (corn stover), 5.34 (rice straw) and 6.25 (reed straw and sugarcane bagasse) (Marriotti *et al.* 2008; Del Rio *et al.* 2015).

Klason Lignin (Acid-insoluble Lignin + Acid-soluble Lignin) Content of Lignin

Determinations of the Klason lignin content of lignin fractions were adapted from TAPPI T222-01 (2011) and TAPPI UM 250 (2000) methods. The acid-insoluble lignin (AIL) was determined gravimetrically as per TAPPI T222 om-11 (2011), and the acid-soluble lignin (ASL) was determined spectrophotometrically according to TAPPI UM 250 (2000).

To determine ASL content, the ultraviolet-visible (UV-Vis) spectrophotometer (Jenway 6315; Cole-Parmer, Roissy Charles de Gaulle, France) was set at a wavelength of 205 nm using 110 g/L cm as the extinction coefficient (ε) for wheat straw lignin (Dominguez-Robles *et al.* 2016), at 240 nm using ε = 25 g/L.cm for sugarcane bagasse lignin (Oriez *et al.* 2019), at 280 nm using ε = 18.5 g/L.cm for reed straw lignin (Faix *et al.* 1989), and at 320 nm using ε = 30 g/L.cm for rice straw and corn stover lignins (Fang *et al.* 2018).

Cellulose and Hemicellulose Content in Lignin

Residual cellulose and hemicellulose contents of lignin fractions were determined based on NREL methods (Sluiter *et al.* 2005, 2008b): The glucose and xylose contained in the fraction were quantified by high-performance liquid chromatography (HPLC; Dionex, Sunnyvale, CA, USA), after chemical hydrolysis. The hydrolysis was conducted in two steps using H_2SO_4: 1.6 mL of H_2SO_4 72 % (12 M) were added to 0.2 g of dry lignin sample and left at room temperature overnight. Then, the mixture was kept at 30 °C for 1 h. After the first step, 22.4 g of distilled water was added, and the mixture was maintained at 120 °C for 1 h.

After the reaction time, the samples were cooled at room temperature before their analysis with HPLC for sugars quantification. The following HPLC conditions were used: Eluent: H_2SO_4 0.005 M; flow rate: 0.6 mL/min; Column Hi-Plex H column (Agilent Technologies, Santa Clara, CA, USA) (300 mm x 7.7 mm), temperature 80 °C; detector refractometer (Shodex Showa Denko, Tokyo, Japan), and a temperature of 50 °C

GPC Analysis

The molecular-average weights of the Biolignin™ samples were determined by GPC. The GPC analyses were carried out on a Waters 1515 Isocratic HPLC pump equipped with a Waters 2414 refractive index detector (Waters, Milford, MA, USA). Three stainless steel columns (Phenogel columns, 300 mm x 7.8 mm x 5 µm, provided by Phenomenex, Torrace, CA, USA) connected in series and packed with a styrene-divinylbenzene copolymer of porosity 100, 500, and 1000 Å, respectively, were used. The following operating conditions were employed: eluent, tetrahydrofuran, THF (Panreac, 99.5%; UV-IR-HPLC-GPC grade, Barcelona, Spain); temperature, 30 °C; sample concentration, 5 mg/mL; injection volume, 20 µL; and flow rate, 1.0 mL/min. Polystyrene (PS) standards used for the GPC calibration curve had molecular weights of: 4910, 3180, 2590, 2170, 1530, 990, 770, 580, and 380 Da. The standards concentration in THF was set at 2 mg/mL.

The Biolignin™ samples were injected without prior derivatization. To limit the presence of insoluble particles in the injected samples, they were previously dissolved in a mixture of 1,4-dioxane/methanol (1:1, v/v, HPLC grade) (Panreac, Barcelona, Spain) to reach a concentration of 40 mg/mL. The solution was then diluted with THF (Panreac, 99.5%; UV-IR-HPLC-GPC grade, Barcelona, Spain) to obtain a final concentration of 10 mg/mL. The solution was then filtrated through a 0.45-µm membrane before analysis. The molecular weight of lignin was quantified relative to polystyrene standards and was therefore not absolute.

^{1}H-^{13}C 2D-NMR Experiments

Prior the analyses, Biolignins™ were esterified with acetic anhydride using the same experimental procedure described in a previous work (Delmas *et al.* 2011).

The NMR experiments were performed at 25 °C on a Bruker Advance 500 MHz (Bruker, Billerica, MA, USA) instrument equipped with a cryogenically cooled 5-mm TCI gradient probe with inverse geometry (5 mm CPTCI 1H-31P/13C Z-GRD Z44913/0001). A total of 125 mg of each acetylated Biolignin™ sample were dissolved in 750 µL of acetone-d_6 (Eurisotop, Saint Aubin, France). Chemical shifts (δ in ppm) were referenced to the carbon (δ_C 29.84 and 206.26 ppm) and the residual proton (δ_H 2.05 ppm) signals of acetone-d_6. The two-dimensional (2D) heteronuclear single quantum coherence (HSQC)-NMR experiments were conducted using Bruker's "hsqcetgpsisp2.2" pulse program (adiabatic-pulsed version) (Bruker, Billerica, MA, USA) with spectral widths of 5341 Hz

(from 10.5 to 0 ppm) and 25,782 Hz (from 206 to 0 ppm) for the ^{1}H- and ^{13}C- dimension, respectively. The number of collection complex points was 2048 for the ^{1}H- dimension with a recycle delay of 1.5 s. The number of transients was 64-, and 256-time increments were always recorded in the ^{13}C- dimension. The $^{1}J_{CH}$ used was 145 Hz. Processing used typical matched Gaussian apodization in the ^{1}H- dimension and squared cosine-bell apodization in the ^{13}C- dimension. Prior to Fourier transformation, the data matrixes were zero-filled up to 1024 points in the ^{13}C- dimension.

The semi-quantitative analysis of the volume integrals (uncorrected) of the HSQC correlation peaks was performed using MestRec 4.9.9.3 processing software (Mestrelab Research, Santiago de Compostela, Spain). This quantitation was conducted following the procedure described by Wen *et al.* (2013) and by Sette *et al.* (2011).

Quantitative ^{31}P NMR Experiment

Approximately 30 mg of each dried lignin sample were transferred into a 1.5-mL sample vial and 400 µL of a mixture of freshly distilled pyridine/ deuterated chloroform (1.6:1, v/v) were added. The sample vial was flushed with Argon gas, sealed, and magnetically stirred at room temperature until complete dissolution.

Chromium (III) acetylacetanoate (99.99%, Sigma Aldrich, St. Louis, MO, USA) and endo-*N*-hydroxy-5-norbornene-2,3-dicarboximide (97%, Sigma Aldrich, St. Louis, MO, USA) were used as the relaxation agent (RA) and internal standard (IS), respectively. A total of 100 µL of 0.1 mmol/mL of the IS and 100 µL of 0.0143 mmol/mL of the RA in the above solvent system were added to the sample vial. Finally, 100 µL of 2-chloro-4,4,5,5-tetramethyl-1,3,2-dioxaphospholane (TMDP) (95%, Sigma Aldrich, St. Louis, MO, USA) was added. The mixture was left at room temperature for 20 min with continuous stirring. The prepared sample solution was then transferred into a 5-mm NMR tube and immediately analyzed. As underlined by Balakshin and Capanema (2015), it is important to quickly analyze the samples after the addition of TMDP, this prevents any deterioration of the internal standard during the NMR experiments.

The spectra were acquired using a Bruker Avance 500 MHz spectrometer (Bruker, Billerica, MA, USA) equipped with a 5-mm TBO BB-1H/31P/D Z-GRD Z104586/0001 probe. A sweep width of 10000 Hz was observed. Spectra were accumulated with time delay of 25 s between pulses. A pulse width causing a 90° flip angle was used. Line broadening of 4 Hz was used in processing spectra. The number of scans was set to 64. All chemical shifts reported in this paper were relative to the reaction product of water with the phosphorylating reagent that has been observed to give a sharp signal in pyridine/$CDCl_3$ at 132.2 ppm (Granata and Argyropoulos 1995). According to previous studies, the maximum standard error of this method is 1.10^{-2} mmol/g and the maximum standard deviation of the results is 2.10^{-2} mmol/g (Jasiukaityte *et al.* 2010).

RESULTS AND DISCUSSION

Yields of Extracted Lignin Fractions (Biolignin™)

The lignin content of the five studied raw materials were determined according to the method developed by the NREL (Sluiter *et al.* 2008). After extraction in organic acid-based media, the yields of recovered lignin-rich fractions are shown in Table 1.

In Table 1, two important data are indicated: The yield of the lignin-rich fraction (Biolignin™) and the yield of the recovered lignin, calculated based on the lignin content

of Biolignin™. It can be noticed for rice straw, that the yield of Biolignin™ was 22.1% when the lignin content of this straw was 19.5%. This can be explained by the relatively low purity of this lignin fraction (80.1%) compared to the other lignin fractions. This is probably due to the high ash content and the high protein content of rice straw compared to the other raw material (see Table 2). In this case more minor compounds were extracted with the lignin, increasing the Biolignin™ yield but decreasing its purity.

The yield of recovered lignin is important since it reflects the process efficiency. Therefore, based on the results (Table 1), which indicate a high lignin recovery in Biolignin™ fractions regardless of the raw material, the CIMV technology can be considered as an optimized process to efficiently fractionate the biomass and extract the lignin. According to the feedstock analysis, sugarcane bagasse contains the highest yield of lignin. However, and even if the SB Biolignin™ is the purest lignin fraction, the rate of recovered lignin from SB is the lowest one. This could be explained by a stronger interaction between lignin fragments and cellulose and/or hemicellulose in bagasse than in the four other biomasses. In fact, in this study, the organosolv process conditions used were basically the same for the five raw materials and were not optimized for each feedstock. A higher lignin recovery rate is expected by optimizing the process conditions to sugarcane bagasse (reaction duration, acids ratio, *etc.*). Indeed, more lignin can be extracted in the acid liquor by increasing the extraction duration, or even by increasing the formic acid rate in the organic acid mixture, in case of more recalcitrant biomass.

Table 1. Yields of Extracted Organosolv Lignins

	Corn Stover	Rice Straw	Wheat Straw	Reed Straw	Sugarcane Bagasse
Feedstock Lignin Content (%)*	19.3	19.5	21.4	23.7	29.7
Biolignin™ Yield*(%)	17.9	22.1	19.3	20.4	19.0
AIL	80.8	77.6	82.8	80.4	87.1
ASL	2.0	2.5	2.5	3.0	3 .0
Lignin in Biolignin™ Fraction (%)	82.8	80.1	85.3	83.4	90.1
Recovered lignin (%)**	76.7	89.0	78.5	77.3	57.6
*of dry biomass, **of total lignin content in biomass					

Chemical Composition of Biolignins™

As seen in Table 1, the Biolignin™ fractions contained from 80 to 90% of lignin, depending on the feedstock. The other minor components were quantitatively determined, including the residual polysaccharides, the proteins, and the mineral content (Table 2).

Table 2. Chemical Composition of Minor Components in Biolignin™ Samples (% per Dry Matter)

	Biolignin™				
	CS	**RS**	**WS**	**ReS**	**SB**
Glucans (%)	1.7	2.3	1.8	0.5	0.4
Standard Deviation (%)	0.2	0.2	0.2	0.1	0.0
Arabinane + Xylane (%)	3.7	2.3	3.7	2.4	2.2
Standard Deviation (%)	0.3	0.5	0.2	0.2	0.1
Ashes (%)	0.9	2.4	0.7	0.6	1.2
Standard Deviation (%)	0.4	1.7	0.3	0.2	0.3
Proteins (%)	9.4	20.7	9.4	3.0	3.7
Standard Deviation (%)	2.3	1.9	0.2	0.4	0.1

The residual polysaccharides content is related to the fractionation process efficiency. When the efficiency increases in the organosolv pretreatment process, the content of C5 and C6 sugars is decreased. Additionally, the residual cellulose and hemicellulose contents are quite low for all the samples, indicating the high efficiency of the fractionation process. Moreover, the residual polysaccharides in lignin fractions can be covalently bonded to the lignin or present as free sugars in the fraction. Therefore, due to the gentle process conditions of the organosolv process, all the lignin-carbohydrate complexes are probably not entirely hydrolyzed.

The minor component distribution in Biolignin™ (other than sugars) is related to the raw material origin. Sugarcane bagasse is a by-product of sugarcane from which the main minor compounds have already been extracted with the sugars. The low amount of minor compounds in SB Biolignin™ is relative to its high amount of Klason lignin (90.1%) compared to the four other Biolignins™.

In the same way, the low percentage of Klason lignin, found in RS Biolignin™ (80.1%), could be explained by the high mineral and proteins composition of rice straw.

The high protein content in RS Biolignin™ (20.7%) was possibly due to the high amount of nitrogen that is not totally in protein form. In fact, some studies highlight that a high amount of nitrogen-rich fertilizers may artificially increase the amount of nitrogen in the biomass: When taken up in excess, N-rich fertilizers are stored as free nitrate in the vacuole of biomass (Umar and Iqbal 2007). However, in the current study, the proteins' N content was calculated from the total N content using the nitrogen-to-protein conversion factor without any distinction between N as amino acid and N as nitrate.

As shown in Table 2, ReS and SB Biolignins™ contain three times less C6 sugar than the other Biolignins™. For SB, the low value of residual C6-sugar can easily be explained by the hot-water pretreatment of the raw material. Indeed, SB is a by-product of sugar industry. The SB was then largely stripped of its C6-sugars before being fractionated by the organosolv pretreatment.

Reed was not deprived of its C6-sugars before its fractionation by the organosolv pretreatment. Then, the low value of C6-sugars in ReS Biolignin™ may indicate the presence a low quantity of covalent bonds between sugars and lignin (Lignin-Carbohydrate complexes). The same process conditions were applied for all the feedstocks (time of extraction, composition of the organic acid media, and temperature). Then, a biomass containing low quantity of C6-sugars/lignins covalent bonds will allow a better separation between lignin and C6-sugars.

Table 3. Inorganic Elemental Composition (ppm per Dry Matter)

Element	Biolignin™				
	CS	**RS**	**WS**	**ReS**	**SB**
Na	59	92	82	42	12
K	96	61	40	50	8
Mg	210	228	202	73	13
Ca	2200	7752	5142	1160	120
Al	320	264	190	17	76
Si	42	638	104	194	320
P	220	385	121	38	77
S	2100	2424	1266	1000	1200
Total	5247	11616	7147	2580	1826

One of the highlights of Table 2 is the high ash contents of RS Biolignin™. This feature is attributed to the high content of silica and calcium of the original plant (Guntzer *et al.* 2012). This trend was confirmed by the elemental composition in Table 3. The main part of inorganic elements contained in the raw materials is extracted in organic acid media and recovered in hemicelluloses fraction. In wheat straw for example, the repartition of the inorganic material in the different fractions is: 80.7% of total ash are recovered in hemicellulose fraction, 8.37% in cellulose fraction, and 0.71% in lignin fraction.

This result is very positive, considering that ash content and its composition may negatively interfere the efficiency of lignin for some applications. For instance, a low amount of mineral compounds is required for lignin-based carbon fibers (Hosseinaei *et al.* 2017; Poursorkhabi *et al.* 2020). Thus, the high ash content of RS Biolignin™ compared to the other samples could be a hindrance for carbon fiber's applications.

Molecular Weight Analysis

In the following, molecular weights of Biolignin™ samples were evaluated to compare the length and the distribution of lignin fragments of each sample.

The molecular weights of Biolignin™ were obtained from a calibration performed with monodisperse polystyrene standards and are considered as relative and not absolute.

Molar mass distribution analysis for lignin is more complex than for many other polymers due to the irregular, polar, and partially branched structure of lignin. This leads to low solubility and partial aggregation when using most GPC solvents. Consequently, GPC provides rather inaccurate results, which limits the possibilities for lignin valorisation and new applications.

The use of a very polar solvent (dimethyl-sulfoxide or dimethyl-formamide) enhances lignin solubility, but increases intramolecular aggregation of lignin oligomers, leading to high molecular weights. Other studies have used derivatized lignins to enhance its solubility in common GPC solvents, such as tetrahydrofuran. The main drawback of derivatization is that it might present conditions for partial degradation or selective recovery of the polymer (Esakkimuthu 2020).

This study employed underived samples instead. Additionally, the solvent mixture was optimized to improve the Biolignin™ sample dissolution. The best results were obtained with the mixture solvent 1,4-dioxane/MeOH/THF (1:1:6 v/v/v). The selected eluent of the GPC system was THF. If lignin content of each sample was considered (*i.e.* Klason lignin), the lignin solubility in the mixture solvent was high enough (*i.e.* > 95 % of lignin solubilized) to obtain reliable molecular weights (Table 4).

Table 4. Molecular Weights Analysis of Biolignin™ Samples

Biolignin ™	M_n (g/mol)	M_w (g/mol)	Polydispersity Index (PDI)	Solubility % (per DM)	Solubility % (per Klason)
RS	1123	2176	1.95	78.0	97.4
CS	1185	2213	1.86	80.0	96.6
WS	1280	2540	1.98	81.7	95.8
ReS	1164	2827	2.44	91.2	100.0
SB	1380	3070	2.22	100.0	100.0

Comparing Biolignin™ of the five annual crops, sugarcane bagasse lignin exhibited the highest molecular weight, followed by wheat straw, reed straw, corn stover, and rice straw lignin. It is commonly accepted that organosolv processses lead to low

molecular weight lignins with less opportunity for repolymerization, as is usually observed in technical lignins (*i.e.*, kraft/alkali process). Within the molecular weight range studied, no noticeable impact of the CIMV organosolv process conditions was found to the molar mass distribution of these five Biolignins™. In this study, the relatively low polydispersity of Biolignin™ samples indicated that whatever the feedstock used, the acid-based organosolv pretreatment extracts lignin with a homogenous distribution of lignin's oligomers. The highest polydispersity was obtained for ReS Biolignin™ (2.44).

^{31}P NMR Analysis

The five Biolignin™ samples were phosphitylated with 2-chloro-4,4,5,5-tetramethyl-1,3,2-dioxaphospholane in the presence of a known amount of endo-*N*-hydroxy-5-norbornene-2,3-dicarboximide as internal standard and submitted to quantitative ^{31}P NMR analyses (Granata and Argyropoulos 1995). The obtained spectra allowed the quantification of different hydroxyl groups (OH), and aromatic carboxylic acids present within the five samples (Table 5). The amounts of aliphatic OH, condensed phenolic OH (5-5' and 4-O-5' condensed G-units), syringyl, guaiacyl, and *p*-hydroxyphenyl phenolic OH (S, G, and H-units), and carboxylic acids were evaluated by integrating the signals in ranges of 150.2 to 144.6, 142.8 to 140.2, 143.7 to 142.2, 140.2 to 138.6, 138.6 to 136.9, and 135.6 to 133.7, respectively.

The ratio of phenolic hydroxyl groups within the analyzed samples was specific for each case. The highest content of *p*-hydroxyphenyl units (H-units) was found in SB Biolignin™ (1.19 mmol/g of Biolignin™), while the lowest one was found in WS Biolignin™ (0.39 mmol/g of Biolignin™). Likewise, ReS Biolignin™ appeared to be the richest sample in S-units (1.21 mmol/g of Biolignin™), while RS Biolignin™ was the sample with the lowest S-units content (0.47 mmol/g of Biolignin™). As is well accepted, the lignin structure is dependent on its origin. Thus, these different ratios of H/G/S units could be directly linked to the origin of the biomass.

In the same way, the aliphatic hydroxyl content, which was higher in wheat straw Biolignin™ than in the other Biolignins™, could be linked to the intrinsic composition of wheat straw lignin.

Then, according to the biomass used, the structure of the lignin recovered by the organic acid-based organosolv pretreatment may be slightly different. For example, even if the total hydroxyl content was almost the same in the ReS and SB Biolignin™ sample (4.66 mmol/g and 4.76 mmol/g, respectively), the ratio aliphatic hydroxyl/phenolic hydroxyl was slightly different: Aliphatic hydroxyl content was 25% higher for RS Biolignin™ (2.10 mmol/g) than for SB Biolignin™ (1.55 mmol/g). In return, phenolic hydroxyl content was 20% higher in SB Biolignin™ (3.21 mmol/g) than in ReS Biolignin™ (2.56 mmol/g).

As underlined by Montiel-Rivera *et al.* (2013) these results might be considered for further chemical modification and/ or applications. For example, the use of a rich aliphatic hydroxyl Biolignin™, as WS Biolignin™, could be a real advantage in polyurethanes synthesis. Indeed, the reactivity of aliphatic hydroxyl groups can be up to 1000 times greater than phenolic hydroxyl, in noncatalyzed reactions with isocyanates at room temperature, mainly due to steric hindrance effects (Antonino *et al.* 2021)

With an average of 0.44 mmol g^{-1}, the amount of carboxylic moieties in the studied Biolignins™ seemed to be higher than in other organosolv lignin references (milled wood lignins, cellulolytic enzymatic lignins, enzymatic mild acidolysis lignins) (Pu *et al.* 2011).

In the study of Pu *et al.* (2011) the average content of carboxylic moieties of extracted lignins was approximately 0.15 mmol g^{-1}.

Lignin naturally contains carboxylic acids, from free benzoic, cinnamic acids, and aliphatic acids (residual hemicelluloses) (Crestini and Argyropoulos 1997). However, the extraction media used in CIMV pretreatment is composed of a mixture of organic acids (formic and acetic acids). This may increase the carboxylic acids' content by cleaving more ester bonds from lignin-lignin and lignin-carbohydrate complexes, as indicated by Moxley *et al.* (2012). The increase of carboxylic acids content in lignins seems to be an indicator of reduction of molecular weight, which also enhances the enzymatic hydrolysis yield (Nakagame *et al.* 2011; Moxley *et al.* 2012). It is noteworthy that this correlation between molecular weight and –COOH content was verified for RS Biolignin™, which showed the highest –COOH content (0.66 mmol.g^{-1}), and the lowest molecular weight.

Table 5. Functional Groups Distribution (mmol/g of sample) in the 5 Biolignins™ Determined by Quantitative ^{31}P NMR Analysis Using 2-Chloro-4,4,5,5-tetramethyl-1,3,2-dioxophospholane as the Phosphiltylating Reagent

Functional Groups (mmol/g of Sample)	RS	CS	WS	ReS	SB
-COOH	0.66	0.55	0.33	0.26	0.42
-OH of H-units	0.46	0.71	0.39	0.65	1.19
-OH of G-units	0.56	0.59	0.74	0.70	0.69
-OH of S-units and Condensed G-units	0.47	0.77	0.81	1.21	1.06
Alk -OH	2.19	2.09	2.34	2.10	1.55
Total -OH	3.68	4.15	4.27	4.66	4.76
Total Alk-OH	2.19	2.09	2.34	2.10	1.55
Total Ar-OH	1.49	2.06	1.93	2.56	3.21

2D- HSQC NMR

Two-dimensional ^{1}H-^{13}C HSQC was employed to obtain additional information on the structure of each of the five organosolv lignins evaluated. Furthermore, to increase the solubility of the samples in deuterated solvent (acetone-d_6), the organosolv lignins were acetylated before measuring the liquid-state NMR experiments. The obtained HSQC spectra can be subdivided into three major regions corresponding to the non-oxygenated aliphatics (δ_C/δ_H 10 to 53/0.8 to 3.0 ppm), the side chains (δ_C/δ_H 40 to 100/3.0 to 6.5 ppm), and the aromatics (δ_C/δ_H 100 to 140/6.0 to 8.0 ppm). As already reported in the literature, no constructive structural information could be drawn from the aliphatic region; therefore the ^{1}H-^{13}C correlations in this region will not be discussed in this study.

The side chains and the aromatics regions of the HSQC spectra are shown in the Supplementary Data (Figs. S1 and S2), the assigned HSQC lignin cross signals are listed in Table 6, and the identified substructures are depicted in Fig. 1. In the following, the bolded numbers refer to the substructures drawn in Fig. 1. The chemical shift assignments of the identified lignin moieties have been assigned by comparison with several previous studies (Ralph *et al.* 2009; Del Rio *et al.* 2012; Zeng *et al.* 2013).

The five Biolignin™ samples could be classified based from the information found in the HSQC spectra as HGS-type lignins. H-units were highlighted by the HSQC correlations between δ_C/δ_H 115/6.3 ppm, and δ_C/δ_H 121/7.5 ppm that mainly correspond to the resonance of aromatics C-3 and C-5 of H-units and between δ_C/δ_H 125/7.0 ppm and δ_C/δ_H 133/7.8 ppm, which could be assigned to the resonance of aromatics C-2 and C-6 of H-units.

Table 6. Assignments of the Lignin ^{13}C-^{1}H (δ in ppm) Correlation Peaks in the 2D HSQC Spectra of the 5 Biolignins™ (Acetone-d_6)

RS		CS		WS		ReS		SB		Assignments (*)
δ_C	δ_H	δ_C	δ_H	δ_C	δ_H	δ_C	δ_H	δ_C	δ_H	
51.6	3.73	51.6	3.74	51.8	3.70	51.6	3.84	51.6	3.75	$C_\beta H$ in phenylcoumaran (β-5') substructure (**2**)
51.2	3.62	51.2	3.60	51.0	3.60	51.8	3.60	51.4	3.60	$C_\beta H$ in 1,2-diarylpropane (β-1') substructure (**4**)
-	-	51.4	2.74	-	-	51.8	2.66	51.4	2.61	$C_\beta H$ in monotetrahydrofuran (α-O-α' and β-β') substructure (**5**)*
-	-	55.3	3.14	55.0	3.13	55.8	3.13	55.3	3.14	$C_\beta H$ in resinol (β-β') substructure (**3**)
63.5	4.36 & 4.53	63.5	4.35 & 4.51	63.2	4.23 & 4.34	64.1	4.38 & 4.53	63.5	4.38 & 4.53	$C_\gamma H_2$ in arylglycerol-β-arylether (β-O-4') substructure linked with G-unit (**1**)
64.5	4.37 & 4.51	64.3	4.38 & 4.48	63.6	4.33 & 4.52	65.3	4.38 & 4.53	64.5	4.37 & 4.51	$C_\gamma H_2$ in 1,2-diarylpropane (β-1') substructure (**4**)
67.8	4.23 & 4.43	67.8	4.27 & 4.42	65.9	4.28 & 4.40	68.5	4.31 & 4.43	67.8	4.30 & 4.44	$C_\gamma H_2$ in phenylcoumaran (β-5') substructure (**2**)
-	-	72.2	3.93 & 4.29	72.0	3.92 & 4.27	73.1	3.91 & 4.28	72.5	3.93 & 4.30	$C_\gamma H_2$ in resinol (β-β') substructure (**3**)
74.8	6.06	75.0	6.06	74.6	6.03	75.2	6.05	75.0	6.05	$C_\alpha H$ in arylglycerol-β-arylether (β-O-4') substructure (**1**)
76.6	6.11	76.6	6.09	76.5	6.09	77.3	6.09	76.8	6.09	$C_\alpha H$ in 1,2-diarylpropane (β-1') substructure (**4**)
-	-	79.7	5.70	79.5	5.69	80.3	5.68	-	-	$C_\alpha H$ in α.β-diarylether (α-O-4' and β-O-4'') substructure (**6**)
81.5	4.71	81.7	4.69	81.1	4.67	82.0	4.71	81.5	4.70	$C_\beta H$ in arylglycerol-β-arylether (β-O-4') substructure (**1**)
-	-	83.2	4.71	84.1	4.76	84.7	4.77	-	-	$C_\beta H$ in α.β-diarylether (α-O-4' and β-O-4'') substructure (**6**)
-	-	84.2	5.17	-	-	84.8	5.17	84.0	5.11	$C_\alpha H$ in monotetrahydrofuran (α-O-α' and β-β') substructure (**5**)*
-	-	86.4	4.76	86.1	4.77	86.9	4.77	86.4	4.77	$C_\alpha H$ in resinol (β-β') substructure (**3**)
88.5	5.65	88.4	5.61	88.1	5.59	89.2	5.63	88.3	5.61	$C_\alpha H$ in phenylcoumaran (β-5') substructure (**2**)
-	-	88.9	6.79	88.5	6.79	89.4	6.80	88.9	6.79	$C_8 H$ in tricin (**9**)
-	-	99.8	6.18	99.7	6.18	100.5	6.19	99.8	6.18	$C_6 H$ in tricin (**9**)
-	-	106.7	7.30	105.9	7.31	107.8	7.32	106.7	7.30	$C_{2'} H$ and $C_{6'} H$ in tricin (**9**)
116.4	6.48	116.4	6.41	116.4	6.49	117.2	6.48	116.6	6.48	$C_\beta H$ in *p*-coumarate and/or ferulate (**8**)
-	-	128.2	6.70	127.4	6.70	128.8	6.70	127.4	6.70	$C_\beta H$ in Cinnamyl aldehyde end groups (**7**)
144.8	7.61	144.6	7.60	144.6	7.63	145.3	7.61	144.8	7.61	$C_\alpha H$ in *p*-coumarate and/or ferulate (**8**)
-	-	153.3	7.61	153.2	7.60	153.9	7.60	153.5	7.59	$C_\alpha H$ in Cinnamyl aldehyde end groups (**7**)
161.5	8.17	161.7	8.13	161.5	8.17	162.4	8.16	161.7	8.14	CH=O of formyl groups
-	-	194.0	9.65	193.6	9.64	195.0	9.65	194.0	9.65	$C_\gamma H$ in Cinnamyl aldehyde end groups (**7**)
** bolded numbers correspond to lignin substructures depicted in Fig. 1*										

The HSQC correlations between δ_C/δ_H 109/6.6 ppm and δ_C/δ_H 115/7.6 ppm and between δ_C/δ_H 121/6.7 ppm and δ_C/δ_H 126/7.8 ppm were mainly attributed to C-2 and C-6 of G-units, respectively. Finally, those between δ_C/δ_H 102/6.2 ppm and δ_C/δ_H 110/7.6 ppm were mainly assigned to C-2 and C-6 of S-units (Fig. S1). The five studied lignins were extracted from herbaceous biomass, thus this HGS composition was expected (Jacquet 1997; Buranov and Mazza 2008). It is known that the biosynthesis of herbaceous lignins induced the metabolization of the three lignin units (H, G, and S) while some other woody biomass, such as softwoods, rarely produced S-units (Lourenço and Pereira 2018).

In addition, as is typical in spectra from grasses, prominent signals corresponding to *p*-coumarate (PCA) and ferulate (FA) structures (**8**) were also observed. The HSQC correlations of the five acetylated samples indicated that the identified *p*-coumarate phenol was free, not etherified. Therefore, these substructures are solely ester linked, as already advanced by other authors (Del Rio *et al.* 2012).

Even if the HGS-type were validated for the five studied Biolignins™, some slight discrepancies could be noted. Lignin extracted from sugarcane bagasse seemed to contain less impurities than the four other samples. This was apparent based on its carbohydrates content, for which the HSQC correlations were less intense than in the other HSQC spectra (anomeric CH of carbohydrates assigned at δ_C/δ_H 101.2/4.88 ppm and signals at δ_C/δ_H 67 to 75/4.6 to 5.6 ppm corresponded to residual carbohydrates in the sample, Fig. S2). The long relaxation times of polysaccharides signals did not allow their quantification in the analyzed lignin samples (Capanema *et al.* 2004). However, a relative comparison of their signal intensity between the five recorded HSQC spectra seemed consistent. The low content of residual carbohydrates in SB Biolignin™ was also underlined by the chemical composition of the lignin samples (See Table 2). In Table 2, the second sample with a relatively low content of carbohydrates was ReS Biolignin™, this is also confirmed by the relatively weak carbohydrate signals on its HSQC spectrum.

Sugarcane bagasse is a by-product of the sugar-refinery industry. In view of the pretreatment undergone by the bagasse, the isolated lignin fraction was expected to be purer than the four other studied lignin samples. As already highlighted by the previous analyses (carbohydrates, proteins, and ashes contents), the HSQC spectrum confirmed the high purity of the recovered organosolv SB lignin fraction.

Nine subunits were identified (Fig. 1). Within these substructures, only three seemed to be contained in the RS Biolignin™ (Table 6), the HSQC correlation signals of the other subunits were under the limit of detection regarding the recording parameters applied.

It was noteworthy to not find any trace of resinol substructures (**3**) in the rice straw lignin sample, while this subunit was distinctly present in the four other samples (*e.g.*, the second most abundant substructure in CS Biolignin™) and is commonly found in herbaceous biomass (Lourenço and Pereira 2018). However, this finding was also revealed by She *et al*. (2012). According to this work, the weak HSQC signals for resinol substructures (**3**) are due to their instability under alkaline conditions. This hypothesis cannot be verified by the present study. Indeed, ^{1}H-^{13}C correlation signals of **3** are well defined in the HSQC spectra of all the analyzed lignin samples except for RS Biolignin™ while all the lignin samples were subjected to the same pretreatment. Thus, in view of these results, the absence of the resinol HSQC signals seemed to be directly linked to the structure of the native lignin in the plant.

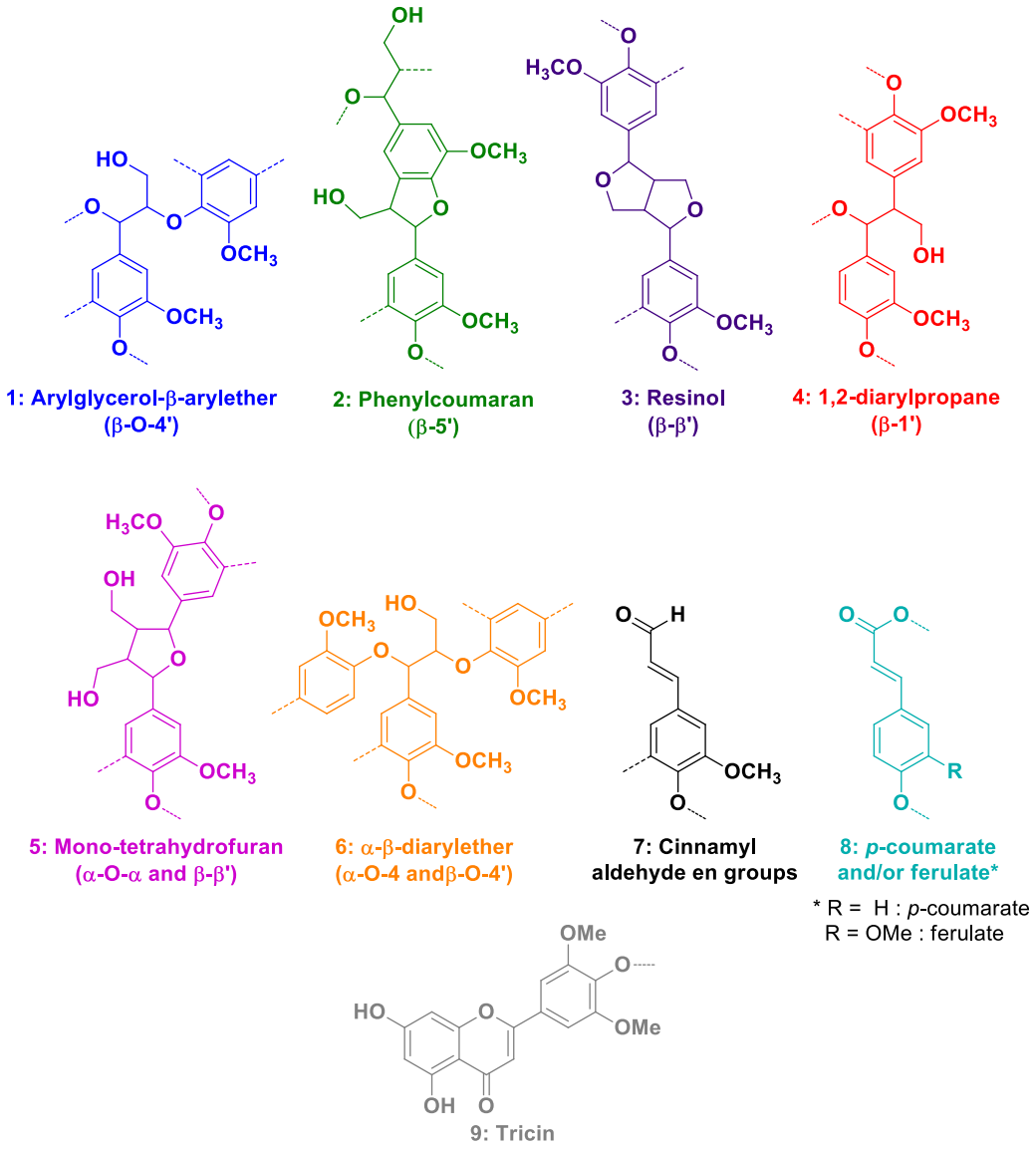

Fig. 1. Main substructures identified in the five organosolv lignin samples

The lignin quantification processed by a combination of ^{13}C and HSQC NMR assumed that the integral of the resonances between 160 and 102 ppm in quantitative ^{13}C NMR contain the total carbon atoms from all aromatic rings within the lignin. Logically, an aromatic ring contributes six carbons; however, the signal of α and β-positions of the vinyl groups in ferulate (**8**), *p*-coumarate (**8**), cinnamyl alcohol, and cinnamyl aldehyde (**7**) also occur in this region and interfere with the overall analysis. To correctly quantify each specific compound, the arylglycerol-*β*-arylether substructure (**1**) was selected as the reference. Thus, the integral of the signal corresponded to $C_\alpha H_\alpha$ of (**1**) was set to **1** (See Table 7). Note that *p*-coumarate and ferulate (**8**) identified in the five lignin samples were not quantified due to the longer relaxation times of these units compared to the rapidly relaxing polymer and the more extensive relaxation the latter experiences during the noticable duration of the pulse experiment itself. Thus, a relative quantitation of these end-units led to an overestimation.

Table 7. Quantification Analysis of the HSQC Side Chain Region by Quantitative HSQC

	RS	CS	WS	ReS	SB
Arylglycerol-β-arylether (β-O-4') Substructure (1)	1 (ref.)	1 (ref.)	1 (ref.)	1 (ref.)	1 (ref.)
Phenylcoumaran (β-5') Substructure (2)	0.26	0.18	0.28	0.11	0.24
Resinol (β-β') Substructure (3)	-	0.21	0.18	0.09	0.21
1,2-diarylpropane (β-1') Substructure (4)	0.11	0.17	0.07	0.19	0.19
Monotetrahydrofuran (α-O-α' and β-β') Substructure (5)	-	0.10	-	0.04	0.03
α.β-diarylether (α-O-4' and β-O-4") Substructure (6)	-	0.01	0.03	0.03	-
Cinnamyl Aldehyde End Groups (7)	-	0.02	0.02	0.04	0.03

The semi-quantitative HSQC analysis indicated that the most abundant substructure of the five lignin samples was arylglycerol-*β*-arylether (**1**, β-O-4' linkage). Only three substructures were identified in RS Biolignin™: arylglycerol-β-arylether (**1**, β-O-4' linkage), more abundant than phenylcoumaran (**2**, β-5' linkage), more abundant than 1,2-diarylpropane (**4**, β-1').

Without considering RS Biolignin™, in which only three substructures were identified, ReS Biolignin™ contained the higher concentration of β-O-4' linkages. Lignin that contain a high amount of β-O-4' linkages are considered as the best candidate for depolymerization due to the lower bond dissociation energy of this linkage (Liu *et al.* 2020).

The three main substructures present in WS and SB Biolignins™ were, from the most to the least abundant: arylglycerol-β-arylether (**1**, β-O-4' linkage), phenylcoumaran (**2**, β-5' linkage), and resinol (**3**, β-β'). These three moieties are largely described in WS and SB lignins (Lino *et al.* 2014; Zikeli *et al.* 2014; Mbotchak *et al.* 2015). For CS Biolignin™ **1**, it was also the substructure with the strongest occurrence, followed by resinol (**3**) and phenylcoumaran (**2**).

As shown in Table 7, monotetrahydrofuran substructure (**5**) is only identified in CS, ReS, and SB Biolignins™. Monotetrahydrofuran substructures are formed by β-β' coupling and subsequent α-O-α' bonding and already identified in nonwoody lignins (Martínez *et al.* 2008). According to the literature, these moieties seem to take part of the biosynthesis of natural acylated lignin fragments (Lu and Ralph 2008).

Finally, some HSQC signals could be attributed to tricin (**9**) in the whole Biolignin™ sample spectra, except those of RS Biolignin™. However, further NMR analyses, such as a heteronuclear multiple bond connectivity (HMBC) experiment are required to confirm its occurrence in the analyzed lignin samples. This moiety was already described in wheat straw lignin (Del Rio *et al.* 2012; Zeng *et al.* 2013).

It is noteworthy that none of the recorded HSQC spectrum showed any trace of lignin moieties, like spirodienone (**10**) and dibenzodioxocin (**11**) (Fig. 2). However, they are frequently described in the literature and represent 0.5 to 3% of the total identified lignin interunit linkages (Del Rio *et al.* 2012; Zeng *et al.* 2013).

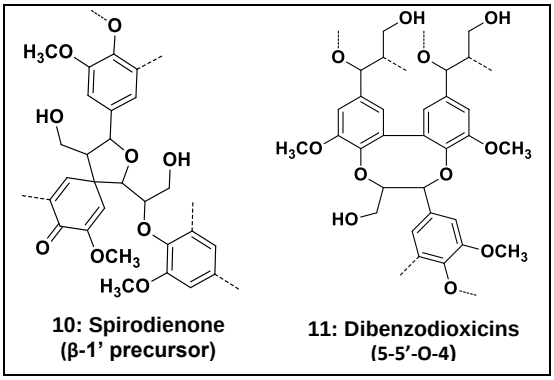

Fig. 2. Lignin moieties frequently found in isolated lignins but absent of the studied samples

CONCLUSIONS

1. With 80 to 90% of Klason lignin in the recovered lignin fractions and with a narrow mass molar distribution, the organosolv pretreatment CIMV is efficient to produce an easily valuable lignin fraction. Similar to what is usually found in herbaceous lignins, the five lignin samples studied were classified as HGS-type lignins.
2. Even if the samples were quite similar, some discrepancies are important to highlight for an optimized valorization. Rice straw Biolignin™ contains a high amount of minerals (Ca and Si). For this reason, some RS Biolignin™ applications, such as carbon fibers substrate, are not possible.
3. ^{31}P NMR revealed that corn stover (CS) and sugarcane bagasse (SB) lignins were rich in non-methoxylated (H-Unit) or mono-methoxylated (G-Unit) phenolic units, making them the best promising candidates for production of phenolic resins. Wheat straw lignin was richer in aliphatic OH than in phenolic OH. This is an advantage for polyurethane synthesis. Reed straw lignin was less specific, with a balanced content of OH groups.
4. 2D HSQC NMR analysis highlighted the high concentration of β-O-4 linkages in ReS lignin, which is an advantage for lignin depolymerization.

ACKNOWLEDGMENTS

The authors thank the CIMV technical team members for their contribution to the experimental data.

REFERENCES CITED

Antonino, L. D., Gouveia, J. R., De Sousa Junior, R. R., Saltarelli Garcia, G. E., Gobbo, L. C., Tavares, L. B., and dos Santos, D. J. (2021). "Reactivity of aliphatic and phenolic hydroxyl groups in kraft lignin towards 4,4' MDI," *Molecules* 26(8), article no. 2131. DOI: 10.3390/molecules26082131

Balakshin, M., and Capanema, E. (2015). "On the quantification of lignin hydroxyl groups with ^{31}P and ^{13}C NMR spectroscopy," *Journal of Wood Chemistry and Technology* 35(3), 220-237. DOI: 10.1080/02773813.2014.928328

Banoub, J. H., Benjelloun-Mlayah, B., Ziarelli, F., Joly, N., and Delmas, M. (2007). "Elucidation of the complex molecular structure of wheat straw lignin polymer by atmospheric pressure photoionization quadrupole time-of-flight tandem mass spectrometry," *Rapid Communications in Mass Spectrometry* 21(17), 2867-2888. DOI: 10.1002/Rcm.3159

Benjelloun-Mlayah, B., and Delmas, M. (2019). "Method of production of lignin and hemicellulose from a plant lignocellulosic material," WIPO Patent No. WO/2019/162277.

Buranov, A. U., and Mazza, G. (2008). "Lignin in straw of herbaceous crops," *Industrial Crops and Products* 28(3), 237-259. DOI: 10.1016/j.indcrop.2008.03.008

Capanema, E. A., Balakshin, M. Y., and Kadla, J. F. (2004). "A comprehensive approach for quantitative lignin characterization by NMR spectroscopy," *Journal of Agricultural and Food Chemistry* 52(7), 1850-1860. DOI: 10.1021/jf035282b

Crestini, C., and Argyropoulos, D. (1997). "Structural analysis of wheat straw lignin by quantitative 31P and 2D NMR spectroscopy. The occurrence of ester bond and α-O-4 substructures," *Journal of Agricultural and Food Chemistry* 45(4), 1212-1219. DOI: 10.1021/jf960568k

De Souza, R. E., Gomes, F. J. B., Brito, E. O., Costa Lelis, R. C., Batalha, L. A. R., Santos, F. A., and Longue, Jr., D. (2020). "A review on lignin sources and uses," *Journal of Applied Biotechnology & Bioengineering* 7(3), 100-105. DOI: 10.15406/jabb.2020.07.00222

Del Rio, J. C., Lino, A., Colodette, J., Lima, C., Gutierrez, A., Martinez, A. T., Lu, F., Ralph, J., and Rencoret, J. (2015). "Differences in the chemical structure of the lignins from sugarcane bagasse and straw," *Biomass and Bioenergy* 81, 322-338. DOI: 10.1016/j.biombioe.2015.07.006

Del Rio, J. C., Rencoret, J., Prinsen, P., Martínez, A. T., Ralph, J., and Gutiérrez, A. (2012). "Structural characterization of wheat straw lignin as revealed by analytical pyrolysis, 2D-NMR, and reductive cleavage methods," *Journal of Agricultural and Food Chemistry* 60(23), 5922-5935. DOI: 10.1021/jf301002n

Delmas, G.-H., Benjelloun-Mlayah, B., Le Bigot, Y., and Delmas, M. (2011). "Functionality of wheat straw lignin extracted in organic acid media," *Journal of Applied Polymer Science* 121(1), 491-501. DOI: 10.1002/app.33592

Delmas, M., Benjelloun-Mlayah, B., and Avignon, G. (2006). "Installation for implementing a method for producing paper pulp, lignins and sugars and production method using such an installation," WIPO Patent No. WO/2006/117295.

Delmas, M. (2008). "Vegetal refining and agrochemistry," *Chemical Engineering and Technology* 31(5), 795-797. DOI: 10.1002/ceat.200800052

Dominguez-Robles, J., Espinosa, E., Savy, D., Rosal, A., and Rodriguez, A. (2016). "Biorefinery process combining Specel® process and selective lignin precipitation using mineral acids," *BioResources* 11(3), 7061-7077. DOI: 10.15376/biores.11.3.7061-7077

Esakkimuthu, E. S. (2020). *Study of New Chemical Derivatization Techniques for Lignin Analysis by Size Exclusion Chromatography*, Ph.D. Dissertation, Grenoble Alpes University, Grenoble, France.

Faix, O., Meier, D., and Beinhoff, O. (1989). "Analysis of lignocelluloses and lignins from *Arundo donax* L. and *Miscanthus sinensis* Anderss., and hydroliquefaction of *Miscanthus*," *Biomass* 18(2), 109-126. DOI: 10.1016/0144-4565(89)90088-7

Fang, S., Wang, W., Tong, S., Zhang, C., and Liu, P. (2018). "Evaluation of the effects of isolated lignin on cellulose enzymatic hydrolysis of corn stover pretreatment by NaOH combined with ozone," *Molecules* 23(6), article no. 1495. DOI: 10.3390/molecules23061495

Granata, A., and Argyropoulos, D. (1995). "2-Chloro-4,4,5,5-tetramethyl-1,3,2-dioxaphospholane, a reagent for the accurate determination of the uncondensed and condensed phenolic moieties in lignins," *Journal of Agricultural Food Chemistry* 43(6), 1538-1544. DOI: 10.1021/jf00054a023

Guntzer, F., Keller, C., and Meunier, J.-D. (2012). "Benefits of plant silicon for crops: A review," *Agronomy for Sustainable Development* 32, 201-213. DOI: 10.1007/s13593-011-0039-8

Hosseinaei, O., Harper, D., Bozell, J., and Rials, D. (2017). "Improving processing and performance of pure lignin carbon fibers through hardwood and herbaceous lignin blends," *International Journal of Molecular Sciences* 18(7), 1410-1423. DOI: 10.3390/ijms18071410

Jacquet, G. (1997). *Structure et Réactivité des Lignines de Graminées et des Acides Phénoliques Associés [Structure and Reactivity of Grass Lignins and Associated Phenolic Acids : Development of Investigation Methodologies]*, Ph.D. Dissertation, Aix Marseille III University, Marseille, France.

Jasiukaityte, E., Kunaver, M., and Crestini, C. (2010). "Lignin behaviour during wood liquefaction-Characterization by quantitative ^{31}P, ^{13}C NMR and size exclusion chromatography," *Catalysis Today* 156(1-2), 23-30. DOI: 10.1016/j.cattod.2010.02.001

Li, M. F., Yang, S., and Sun, R. C. (2016). "Recent advances in alcohol and organic acid fractionation of lignocellulosic biomass," *Bioresource Technology* 200, 971-980. DOI: 10.1016/j.biortech.2015.10.004

Lino, A., Rencoret, J. G., Colodette, J., Lima, C., Martinez, A., and Del Rio, J. (2014). "Structural characterization of the lignins from sugarcane bagasse and straw," in: *13th European Workshop on the Lignocellulosics and Pulp*, Seville, Spain, pp. 519-522.

Liu, X., Bouxin, F. P., Fan, J., Budarin, V. L., Hu, C., and Clark J. H. (2020). "Recent advances in the catalytic depolymerization of lignin towards phenolic chemicals: A review," *ChemSusChem* 13(17), 4296-4317. DOI: 10.1002/cssc.202001213

Lourenço, A., and Pereira, H. (2018). "Compositional variability of lignin in biomass," in: *Lignin Trends and Applications*, M. Poletta (Éd.), IntechOpen, Rijeka, Croatia, pp. 65-98. DOI: 10.5772/intechopen.71208

Lu, F., and Ralph, J. (2008). "Novel tetrahydrofuran structures derived from β-β coupling reactions involving sinapyl acetate in kenaf lignins," *Organic & Biomolecular Chemistry* 6(20), 3681-3694. DOI: 10.1039/b809464k

Marriotti, F., Tomé, D., and Mirand, P. (2008). "Converting nitrogen into proteins - Beyond 6.25 and Jones' factors," *Critical Reviews in Food Science and Nutrition* 48(2), 177-184. DOI: 10.1080/10408390701279749

Martínez, A. T., Rencoret, J., Marques, G., Gutiérrez, A., Ibarra, D., Jiménez-Barbero, J., and Del Rio, J. C. (2008). "Monolignol acylation and lignin structure in some nonwoody plants: A 2D NMR study," *Phytochemistry* 69(16), 2831-2843. DOI: 10.1016/j.phytochem.2008.09.005

Mbotchak, L., Le Morvan, C., Duong, K. L., Rousseau, B., Tessier, M., and Fradet, A. (2015). "Purification, structural characterization, and modification of organosolv wheat straw lignin," *Journal of Agricultural and Food Chemistry* 63(21), 5178-5188. DOI: 10.1021/acs.jafc.5b02071

Montiel-Rivera, F., Phuong, M., Ye, M., Halasz, A., Hawari, J. (2013). "Isolation and characterization of herbaceous lignins for applications in biomaterials," *Industrial Crops and Products* 41, 356-464. DOI: 10.1016/j.indcrop.2012.04.049

Moxley, G., Gaspar, A. R., Higgins, D., and Xu, H. (2012). "Structural changes of corn stover lignin during acid pretreatment," *Journal of Industrial Microbiology and Biotechnology* 39(9), 1289-1299. DOI: 10.1007/s10295-012-1131-z

Nakagame, S., Chandra, R. P., Kadla, J. F., and Saddler, J. N. (2011). "Enhancing the enzymatic hydrolysis of lignocellulosic biomass by increasing the carboxylic acid content of associated lignin," *Biotechnology and Bioengineering* 108(3), 538-548. DOI: 10.1002/bit.22981

Oriez, V., Peydecastaing, J., and Pontalier, P.-Y. (2019). "Separation of sugarcane bagasse mild alkaline extract components by ultrafiltration- membrane screening and effect of filtration parameters," *Process Biochemistry* 78, 91-99. DOI: 10.1016/j.procbio.2019.01.006

Pan, X., and Sano, Y. (1999). "Atmospheric acetic acid pulping of rice straw IV: Physicochemical characterization of acetic acid lignins from rice straw and woods. Part 1. Physical characteristics," *Holzforschung* 53(5), 511-518. DOI: 10.1515/HF.1999.084

Poursorkhabi, V., Abdelwahab, M. A., Misra, M., Khalil, H., Gharabaghi, B., and Mohanty, A. K. (2020). "Processing, carbonization, and characterization of lignin based electrospun carbon fibers: A review," *Frontiers in Energy Research* 8, article mo. 208. DOI: 10.3389/fenrg.2020.00208

Poveda-Giraldo, J. A., Solarte-Toro, J. C., and Cardona Azate, C. A. (2021). "The potential use of lignin as a platform product in biorefineries: A review," *Renewable and Sustainable Energy Reviews*, 138, 110688. DOI: 10.1016/j.rser.2020.110688

Pu, Y., Cao, S., and Ragauskas, A. J. (2011). "Application of quantitative 31P NMR in biomass lignin and biofuel precursors characterization," *Energy & Environmental Science* 4(9), 3154-3166. DOI: 10.1039/c1ee01201k

Ralph, J., Lundquist, K., Brunow, G., Lu, F., Kim, H., Schatz, P. F., Marita, J. M., Hatfield, R. D., Ralph, S. A., Christensen, J. H., *et al.* (2004). "Lignins: Natural polymers from oxidative coupling of 4-hydroxyphenyl-propanoids," *Phytochemistry Reviews* 2004(3), 29-60. DOI: 10.1023/B:PHYT.0000047809.65444.a4

Ralph, S. A., Ralph, J., and Landucci, L. L. (2009). "NMR Database of lignin and cell wall model compounds," (www.glbrc.org/databases_and_software/nmrdatabase/), Accessed 01 March 2021.

Sette, M., Wechselberger, R., and Crestini, C. (2011). "Elucidation of lignin structure by quantitative 2D NMR," *Chemistry - A European Journal* 17(34), 9529-9535. DOI: 10.1002/chem.201003045

She, D., Nie, X. N., Xu, F., Geng, Z. C., Jia, H. T., Jones, G. L., and Baird, M. S. (2012). "Physico-chemical characterization of different alcohol-soluble lignins from rice straw," *Cellulose Chemistry and Technology* 46(3-4), 207-219.

Sluiter, A., Hames, B. Ruiz, R., Scarlata, C., Sluiter, J., and Templeton, D. (2008a). *Determination of Ash in Biomass* (NREL/TP-510-42622), National Renewable Energy Laboratory, Golden, CO, USA.

Sluiter, A., Hames, B. Ruiz, R., Scarlata, C., Sluiter, J., Templeton, D., and Crocker, D. (2008b). *Determination of Structural Carbohydrates and Lignin in Biomass* (NREL/TP-510-42628), National Renewable Energy Laboratory, Golden, CO, USA.

Sluiter, A., Ruiz, R., Scarlata, C., Sluiter, J., and Templeton, D. (2005). *Determination of Extractives in Biomass* (NREL/TP-510-42619), National Renewable Energy Laboratory, Golden, CO, USA.

Snelders, J., Dornez, E., Benjelloun-Mlayah, B., Huijgen, W. J. J., de Wild, P. J., Gosselink, R. J. A., Gerritsma, J., and Courtin, C. M. (2014). "Biorefining of wheat straw using an acetic and formic acid based organosolv fractionation process," *Bioresource Technology* 156, 275-282. DOI: 10.1016/j.biortech.2014.01.069

TAPPI T222 om-11 (2011). "Acid-insoluble lignin in wood and pulp," TAPPI Press, Atlanta, GA, USA.

TAPPI UM 250 (2000). "Acid-soluble lignin in wood and pulp," TAPPI Press, Atlanta, GA, USA

Thoresen, P. P., Matsakas, L., Rova, U., and Christakopoulos, P. (2020). "Recent advances in organosolv fractionation. Toward biomass fractionation technology of the future," *Bioresource Technology* 306, article ID 123189. DOI: 10.1016/j.biortech.2020.123189

Umar, A., and Iqbal, M. (2007). "Nitrate accumulation in plants, factors affecting the process, and human health implication. A review," *Agronomy for Sustainable Development* 27, 45-57. DOI: 10.1051/agro:2006021

Vishtal, A., and Kraslawski, A. (2011). "Challenges in industrial applications of technical lignins," *BioResources* 6(3), 3547-3568. DOI: 10.15376/biores.6.3.vishtal

Watkins, D., Nuruddin, M., Hosur, M., Tcherbi-Narteh, A., and Jeelani, S. (2015). "Extraction and characterization of lignin from different biomass resources," *Journal of Materials Research and Technology* 4(1), 26-32. DOI: 10.1016/j.jmrt.2014.10.009

Wen, J.-L., Sun, S.-L., Xue, B.-L., and Sun, R.-C. (2013). "Recent advances in characterization of lignin polymer by solution-state nuclear magnetic resonance (NMR) methodology," *Materials* 6(1), 359-391. DOI: 10.3390/ma6010359

Zeng, J., Helms, G., Gao, X., and Chen, S. (2013). "Quantification of wheat straw lignin structure by comprehensive NMR analysis," *Journal of Agricultural and Food Chemistry* 61(46), 10848-10857. DOI: 10.1021/jf4030486

Zikeli, F., Ters, T., Fackler, K., Srebotnik, E., and Li, J. (2014). "Successive and quantitative fractionation and extensive structural characterization of lignin from wheat straw," *Industrial Crops and Products* 61, 249-257. DOI: 10.1016/j.indcrop.2014.07.013

Article submitted: June 25, 2021; Peer review completed: August 22, 2021; Revised version received and accepted: September 6, 2021; Published: October 14, 2021.
DOI: 10.15376/biores.16.4.7966-7990

APPENDIX

Supplementary Data

In the following, Fig. S1 represents the aromatic region of the HSQC spectra of the five acetylated Biolignin™ samples where H, G, and S-units are highlighted. The side chain region of the HSQC spectra is shown in Fig. S2. The correlation plots of the identified substructures are indicated.

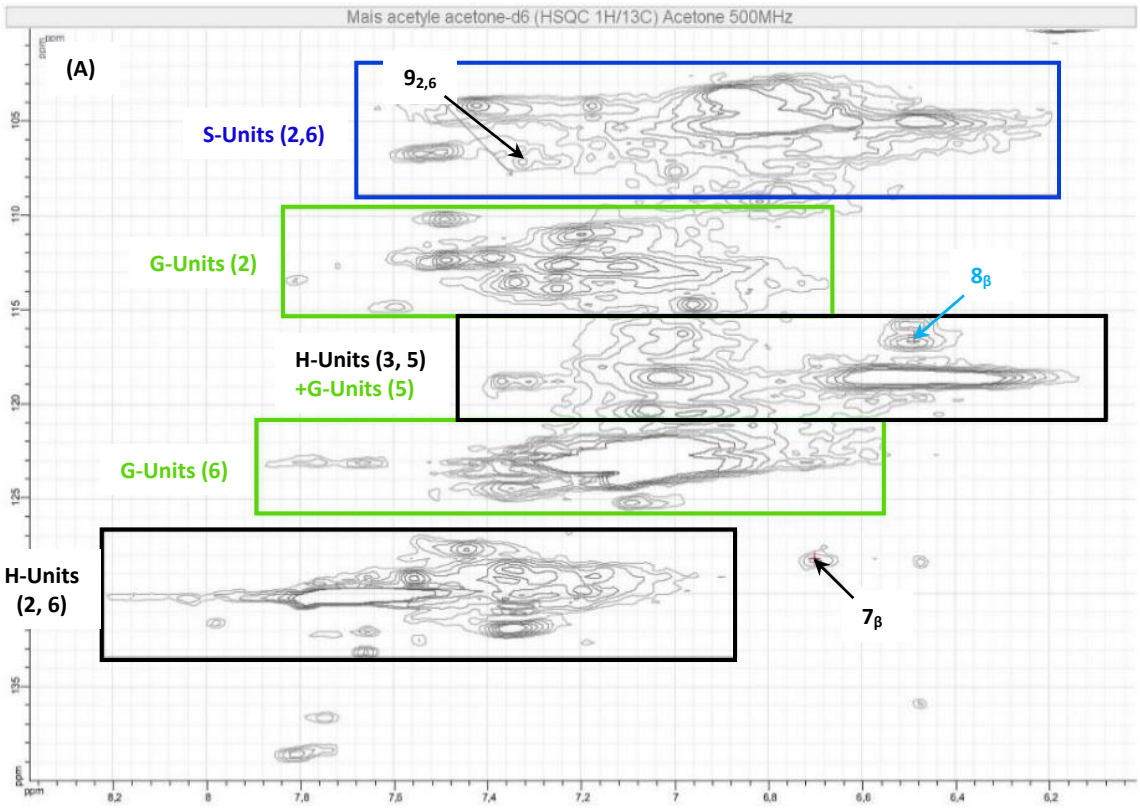

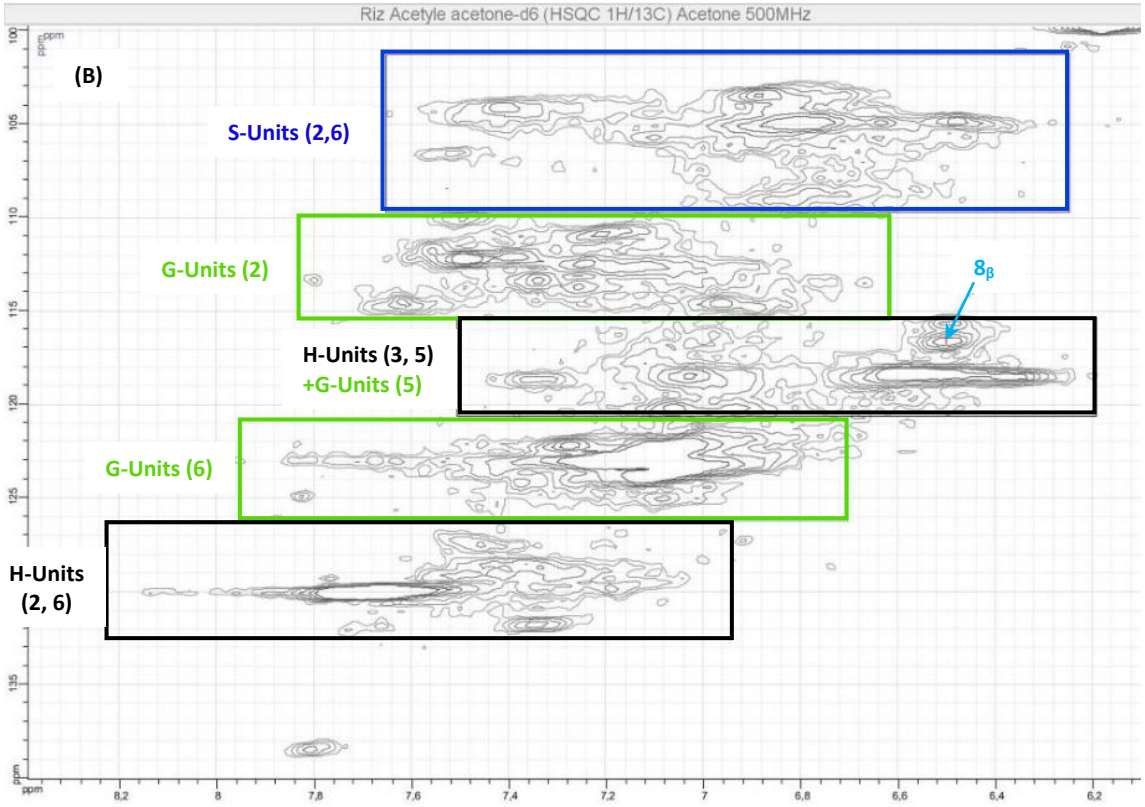
Riz Acetyle acetone-d6 (HSQC 1H/13C) Acetone 500MHz
(B)
S-Units (2,6)
G-Units (2)
8β
H-Units (3, 5)
+G-Units (5)
G-Units (6)
H-Units
(2, 6)

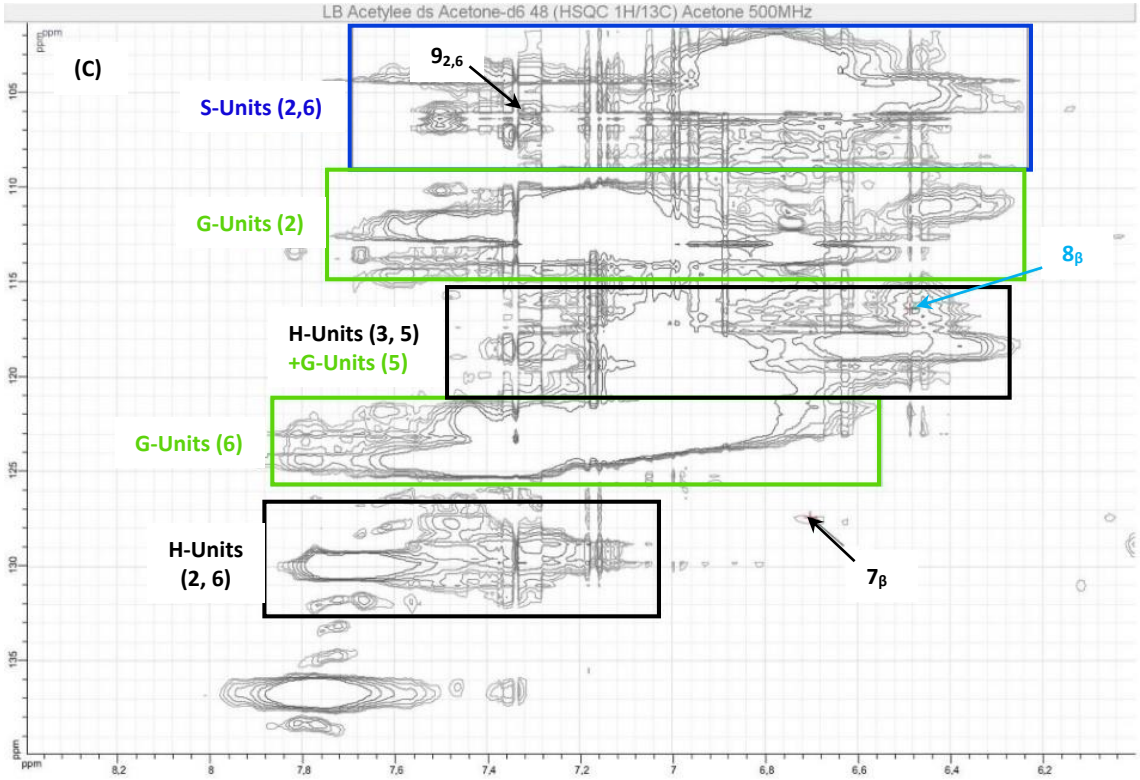
LB Acetylee ds Acetone-d6 48 (HSQC 1H/13C) Acetone 500MHz
(C)
9₂,₆
S-Units (2,6)
G-Units (2)
8β
H-Units (3, 5)
+G-Units (5)
G-Units (6)
H-Units
(2, 6)
7β

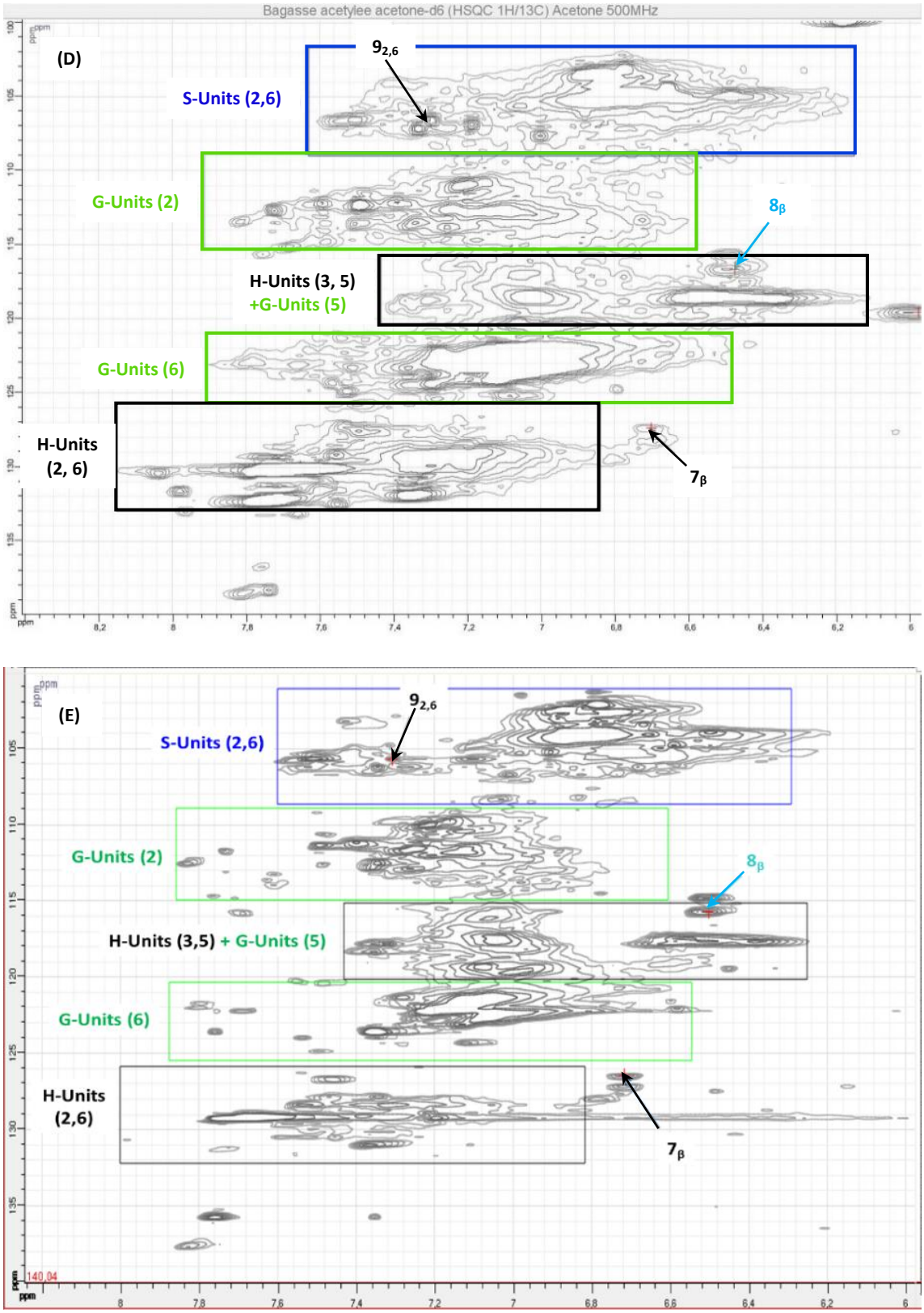

Fig. S1. Aromatics region of the HSQC spectra of acetylated corn straw (A), rice straw (B), wheat straw (C), sugarcane bagasse (D), and reed straw (E) Biolignin™ samples (Acetone-d_6)

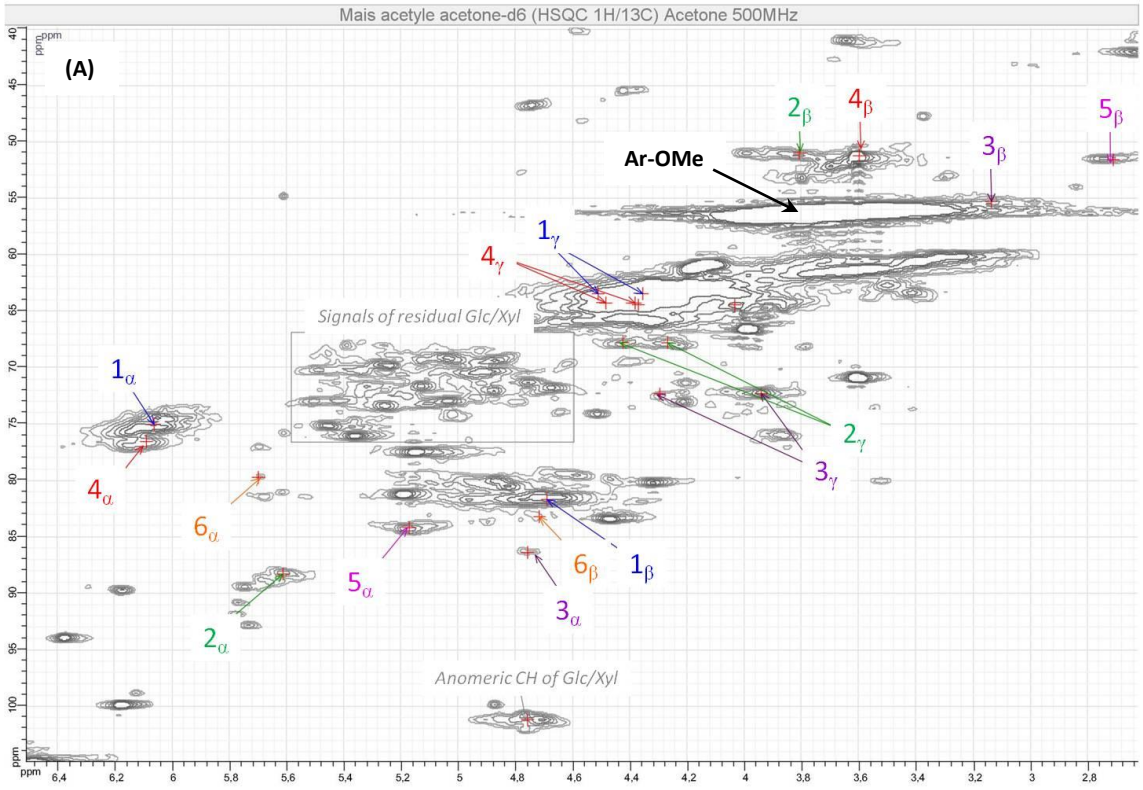
Mais acetyle acetone-d6 (HSQC 1H/13C) Acetone 500MHz
(A)
Ar-OMe
Signals of residual Glc/Xyl
Anomeric CH of Glc/Xyl

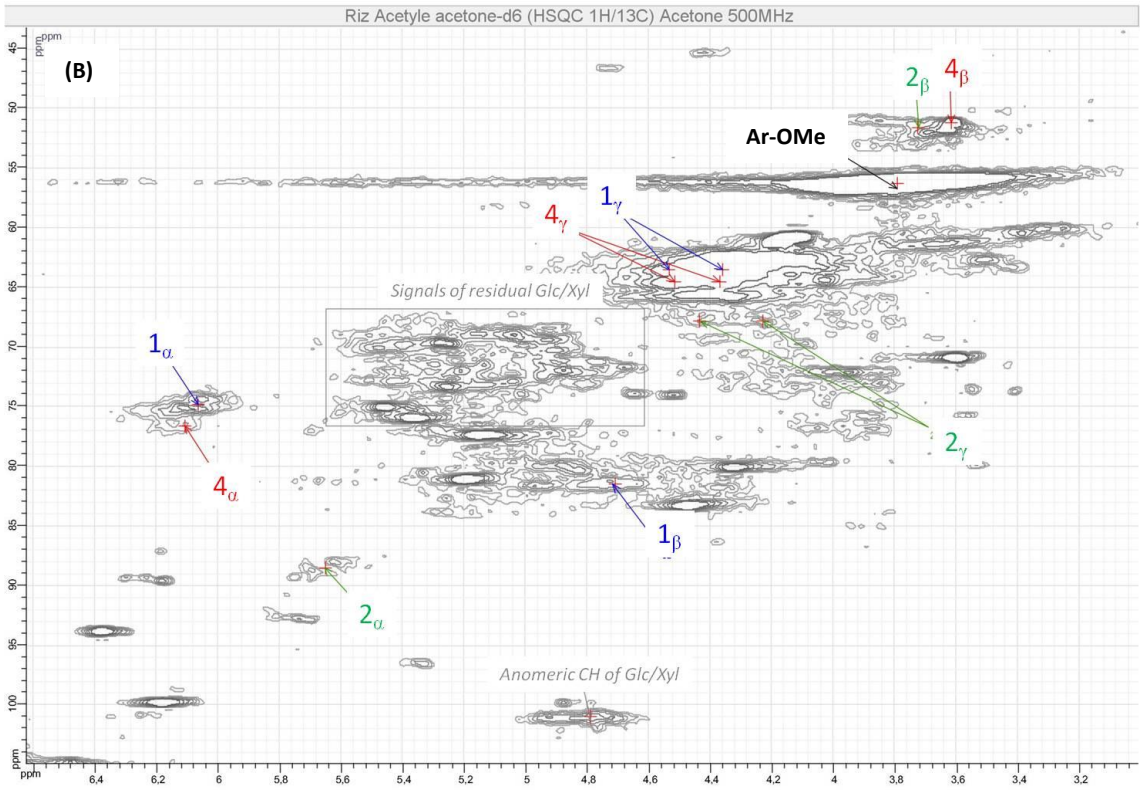
Riz Acetyle acetone-d6 (HSQC 1H/13C) Acetone 500MHz
(B)
Ar-OMe
Signals of residual Glc/Xyl
Anomeric CH of Glc/Xyl

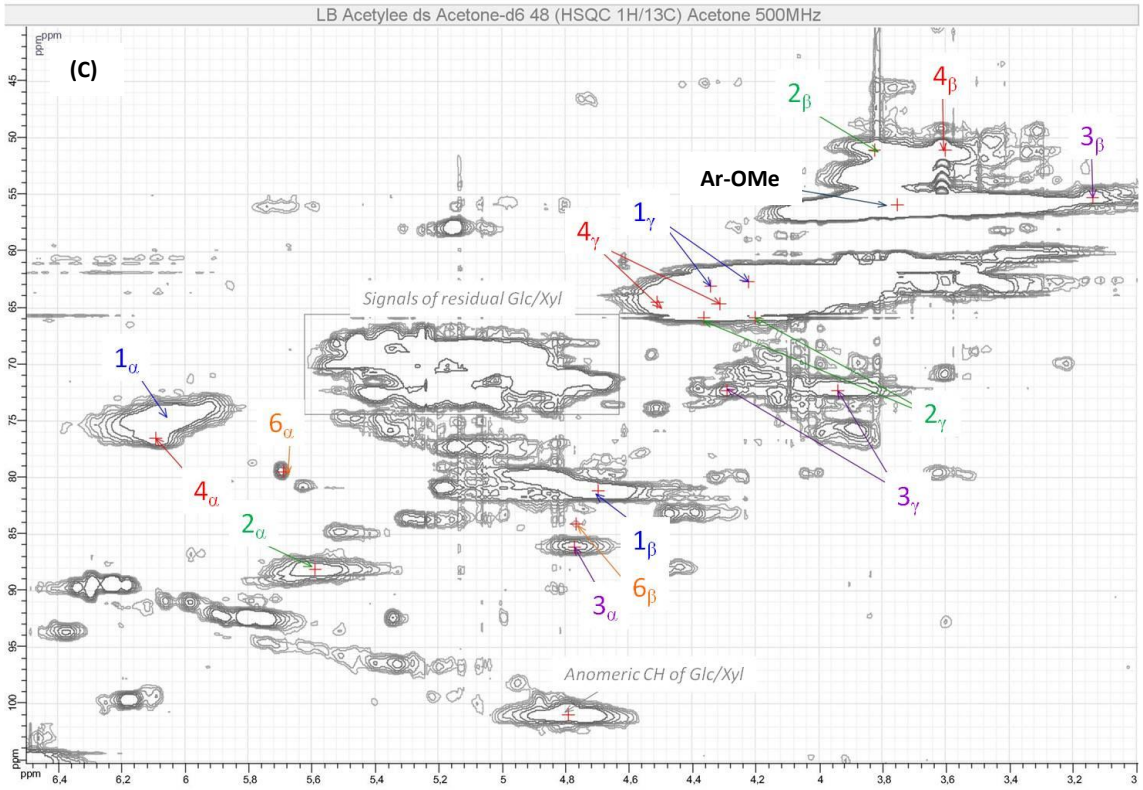
LB Acetylee ds Acetone-d6 48 (HSQC 1H/13C) Acetone 500MHz
(C)
Ar-OMe
Signals of residual Glc/Xyl
Anomeric CH of Glc/Xyl

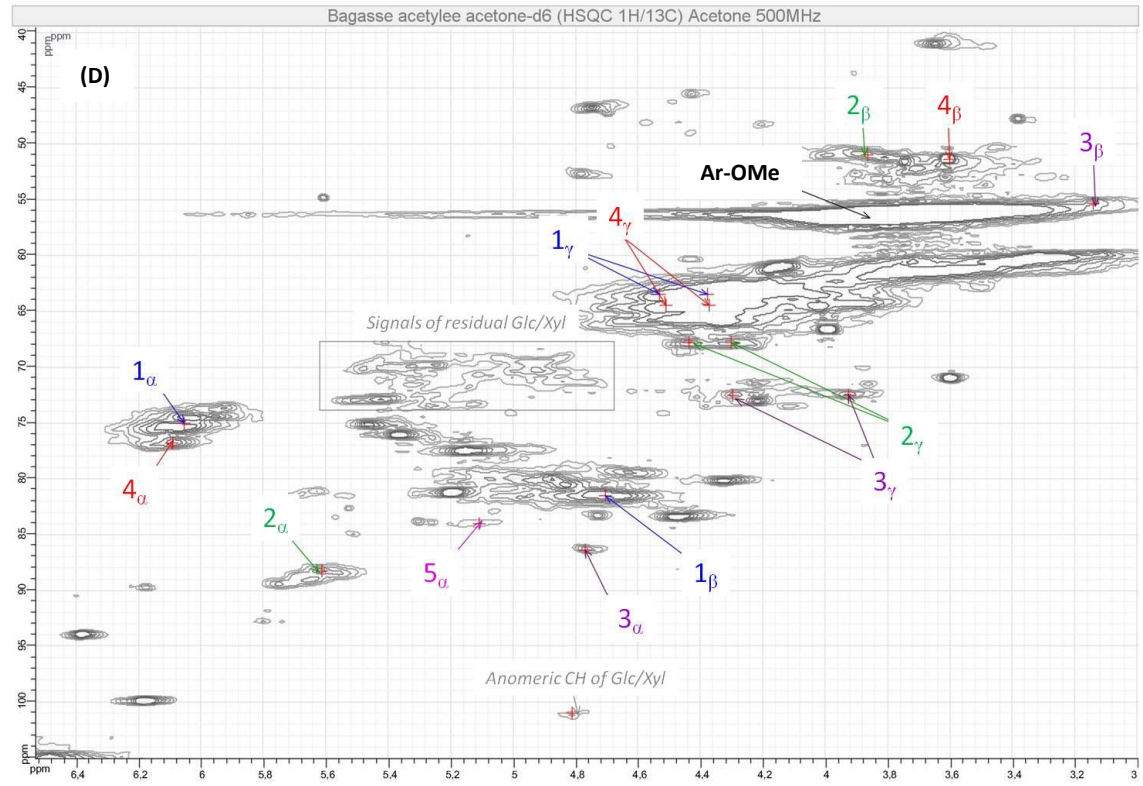
Bagasse acetylee acetone-d6 (HSQC 1H/13C) Acetone 500MHz
(D)
Ar-OMe
Signals of residual Glc/Xyl
Anomeric CH of Glc/Xyl

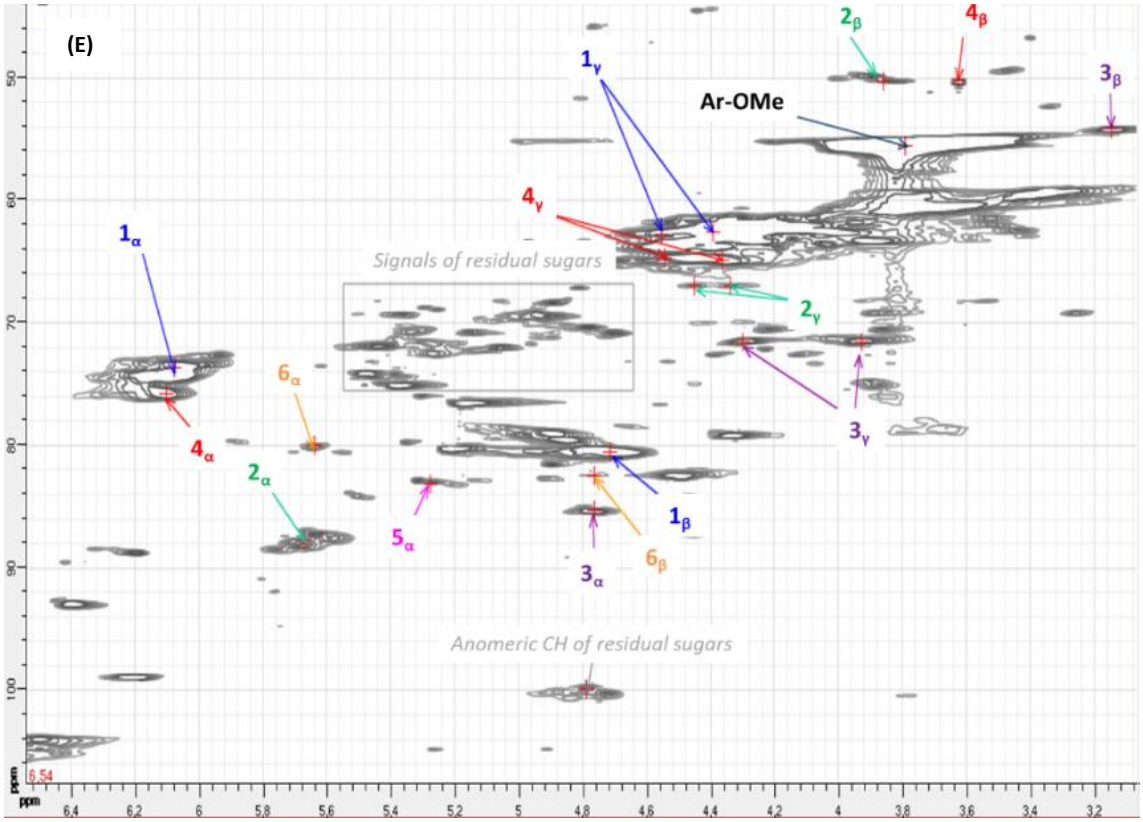

Fig. S2. Side chain region of the HSQC spectra of acetylated corn straw (A), rice straw (B), wheat straw (C), sugarcane bagasse (D), and reed straw (E) Biolignin^{TM} samples (Acetone-d_6)